Flow in a shock tube

May 12, 2020

1 Summary

In this lab, a shock tube is used as a supersonic wind tunnel to study the flow around a wedge. The experiments are performed for three different flow Mach numbers by changing the pressure ratios of the driver and driven sections, which are split initially by a Fast Opening Valve. The required pressure ratios are calculated before the experiments and the flow Mach numbers are verified from pressure measurements. The flow Mach number is further verified from the shock angle when oblique shocks form around the wedge.

2 Wave motion in a shock tube

The theoretical calculations are based on idealised shock tube flow. This incorporates the following assumptions:

- Ideal gases in driver and driven section
- Instant opening of the valve
- Adiabatic and friction-less flow

The shock tube is initially split into a driver (high pressure) and driven (low pressure) sections by a Fast Opening Valve (FOV). Figure 1 shows the wave motion inside the shock tube after the FOV opening.

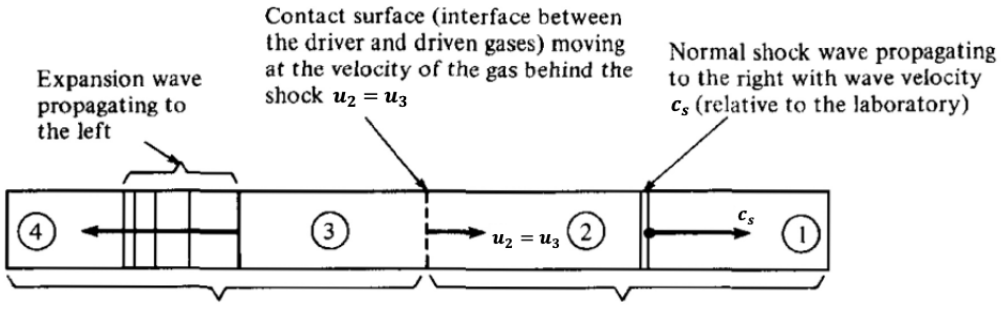

Figure 1: Wave motion inside the shock tube after the Fast Opening Valve (FOV) opening. Adapted from Ref. [1]

.

Figure 2 is the $x-t$ diagram of the shock tube with the wedge inside, before any reflections of the waves happen in the tube. Figure 1 corresponds to the time, t, in Figure 2. The descriptions of different states are as follows:

a. When the FOV opens, a rapid depressurisation of the driver leads to the formation of a *shock wave* propagating through the driven section. The normal shock relation holds across this incident shock wave and it splits the states 1 and 2.

b. At the same time, *expansion waves* are formed and propagate to the opposite direction through the driver section. This expansion fan is isentropic and splits the states 3 and 4.

c. Between the shock wave and the expansion fan, there is an interface of driver and driven gases. This is called the *contact surface* and it splits the states 2 and 3. The two gases are moving at the same speed, hence the pressure and the velocity are the same across the contact surface. However, being an interface of the two gases, it is a discontinuity of the temperature and the density.

d. When the shock wave and the expansion fan reach the end walls, they reflect and interactions between the different waves are initiated. Then, it is difficult to estimate the gas properties using the idealised shock tube flow relations.

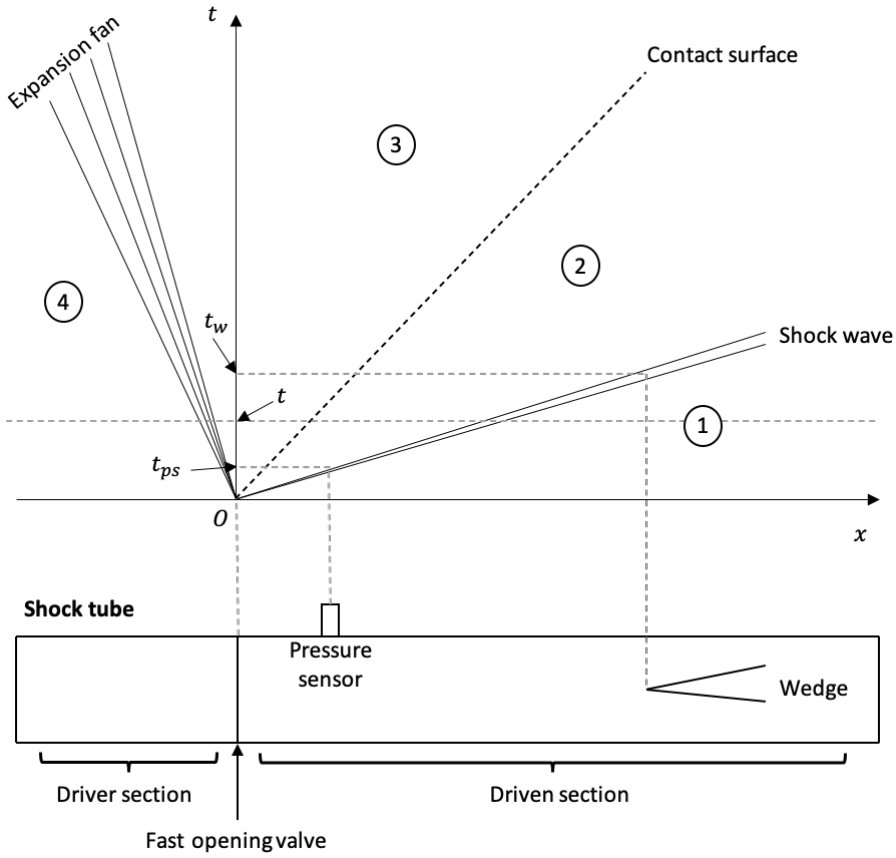

Figure 2: $x-t$ diagram of the waves inside the shock tube before reflections

To study the flow around the wedge for different Mach numbers, the Mach number in state 2, M_2, is varied by changing the pressure ratio p_4/p_1. The two can be related through the incident shock Mach number, M_s.

The continuity, momentum and energy equations across the incident shock wave can be written as:

$$\rho_1 c_s = \rho_2 (c_s - u_2),$$
$$p_1 + \rho_1 c_s^2 = p_2 + \rho_2 (c_s - u_2)^2,$$
$$h_1 + \frac{c_s^2}{2} = h_2 + \frac{c_s - u_2^2}{2},$$

where ρ, u, p and h are the density, velocity, pressure and enthalpy, respectively. c_s is the velocity of the incident shock wave. The numbers in subscripts correspond to the states in the shock tube. Together with the normal shock jump relations, M_2 can be derived as a function of M_s

$$M_2 = \frac{2(M_s^2 - 1)}{[2\gamma_1 M_s^2 - (\gamma_1 - 1)]^{\frac{1}{2}} [(\gamma_1 - 1) M_s^2 + 2]^{\frac{1}{2}}}.$$

Considering the boundary conditions of each wave mentioned in the points a to d previously, the relationship between p_4/p_1 and M_s is expressed as

$$\frac{p_4}{p_1} = \frac{2\gamma_1 M_s^2 - (\gamma_1 - 1)}{\gamma_1 + 1} \left[1 - \frac{\gamma_4 - 1}{\gamma_1 + 1} \frac{a_1}{a_4} \left(M_s - \frac{1}{M_s} \right) \right]^{-\frac{2\gamma_4}{\gamma_4 - 1}},$$

where γ and a are the heat capacity ratio and speed of sound.

3 Experimental rig and apparatus

The setup of the experiment is sketched in Figure 3.

The total length of the shock tube is approximately 4 m and it has a rectangular cross-section of 50 x 120 mm. The driver section may go up to 32 bar (limited for safety reasons) and the driven section can be evacuated down to 0.01 bar. The two are separated by a Fast Opening Valve (FOV). In classical shock tube setups, thin aluminium or plastic membranes are ruptured to create shocks instead of the FOV. However, the pressure ratio p_4/p_1 is related to the membrane material and thickness, whereas with the FOV, any pressure ratio can be realised within the range of specifications. Usage of the membranes is generally more time consuming: they have to be replaced for every experiment, the rupture could be inconsistent and the debris may cause damage to the test models. These may degrade the quality of the experiments. Therefore, the FOV is adopted in the KTH shock tube. The downside of the FOV is that although its opening time is in the order of milliseconds, it requires relatively longer time for the shock to fully form compared to the membranes. This finite time in shock formation causes the p_4/p_1 to M_s relation to deviate from the theory where instant shock formation was assumed. The theoretical relations only hold from the point where the incident shock has fully formed (see Figure 4). Given the larger volume, in the actual experiment, more gas has to be pumped into the driver section to match the *effective* p_4 to the theoretical p_4. This is true for both membranes and FOVs, but since the deviation is larger for the FOVs, it is convenient to have a calibration curve of p_4/p_1 versus M_s for a given facility. The curve for the KTH shock tube is shown in Figure 6.

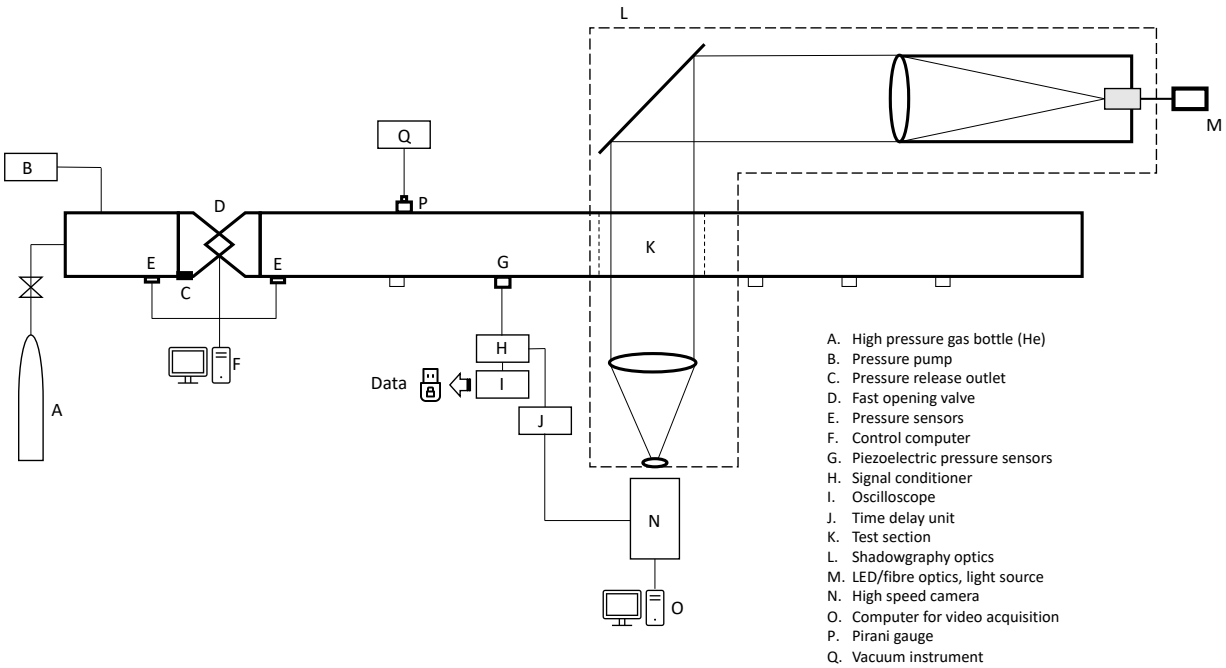

Figure 3: Schematic of the shock tube and the data acquisition system.

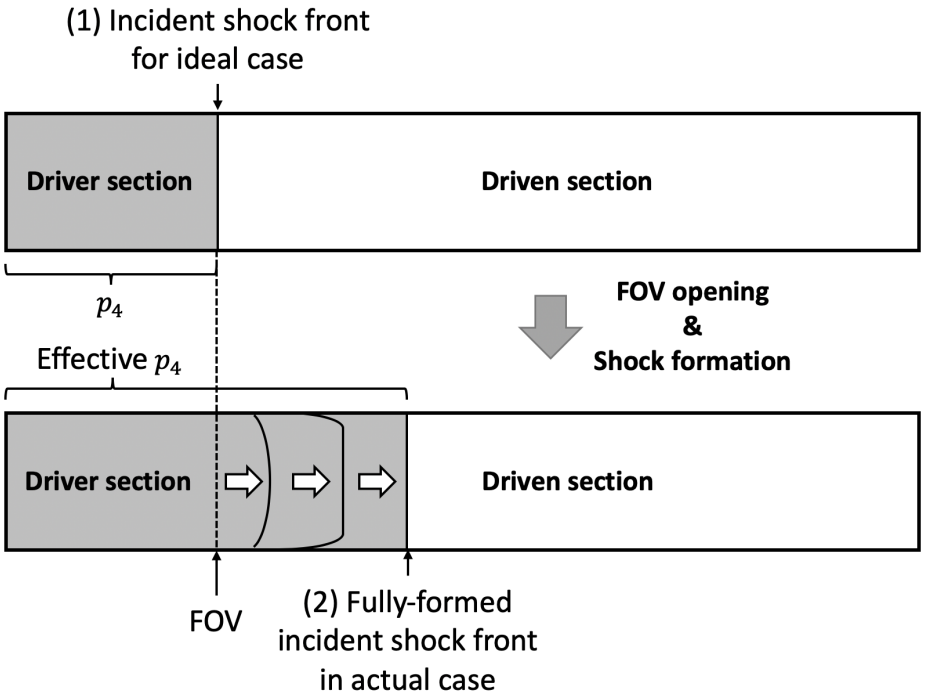

Figure 4: Shock formation in ideal case (1) and actual case (2).

The test section is located approximately 2.5 m downstream of the FOV to allow the shock wave to fully form before reaching the wedge. To increase the test time, there is another metre after the test section which delays the arrival of reflected shock wave at the wedge. This ensures a steady condition behind the incident shock wave for a finite time, making it possible to analyse the flow around the wedge.

The driver gas is supplied from a high-pressure gas bottle with a pressure regulating valve. The driven section is evacuated by a two-stage vacuum pump to below atmospheric level, to effectively increase the pressure ratio. A computer programme controls and regulates these pressures, and opens the FOV at a predetermined pressure ratio. In this laboratory exercise, helium is used in the driver and air in the driven section. The properties of the used gases are found in Table 1. After evacuating the air in the driven section, ambient air is jet in through a valve and the section is evacuated again to the right pressure level. This is done for each experiment to ensure that there is no helium left from the previous experiment inside the driven section.

Table 1: Properties of ideal gas at 300 K

	Heat capacity ratio, γ [-]	Gas constant, R [J/kg · K]
Air	1.400	287.058
Helium	1.667	2076.90

The driven section of the tube is equipped with a number of sensor ports on the side wall. A piezoelectric pressure sensor (PCB 113B28) is placed 54 cm upstream of the leading edge of the wedge. The sensor is composed of a diaphragm and quartz plates. When a certain material, in this case the quartz, is exposed to a mechanical stress, it produces some voltage. This is called the *piezoelectric effect* ("piezo" from Greek: "to squeeze"). The surface of the diaphragm is mounted flush with the inner wall of the tube. As the shock passes over the sensor, the jump in pressure deforms the diaphragm, which pushes the quartz plates together, and generates a corresponding voltage. The sensor is very fast and the response time is less than 1 μs, making it an ideal sensor for such dynamic measurements. Its signal is passed to the oscilloscope via a signal conditioner.

The wedge is mounted inside the test section, downstream of the pressure sensor. It has two angles, 8° at the top and 4° at the bottom. To facilitate optical access, the test section has vertical plexiglass windows. The wedge is levelled in the middle of the cross-section and mounted normal to the plexiglass surfaces. Shadowgraph technique is used to visualise the oblique shock at the wedge. A fibre-coupled LED light is used to create the continuous, single-point light source. The light is passed through a converging lens to obtain a parallel beam. It is then directed into the test section by a mirror. It passes through a second lens and another focusing lens to obtain a sufficient field of view at the high speed camera. The schematic of the setup is shown in Figure 5 and the specific optical setup for this experiment is found in Figure 3. More details are provided in the book chapter [2] for interested students, uploaded as "Merzkirch-Egami_2007.pdf". The camera is triggered by the pressure sensor. The starting of the video recording is delayed by a certain time which depends on the experiments, but the time counter at the bottom-right corner on the video is always triggered by the pressure sensor *i.e.* "0 ns" is when the incident shock has passed over the pressure sensor (t_{ps} in Figure 2).

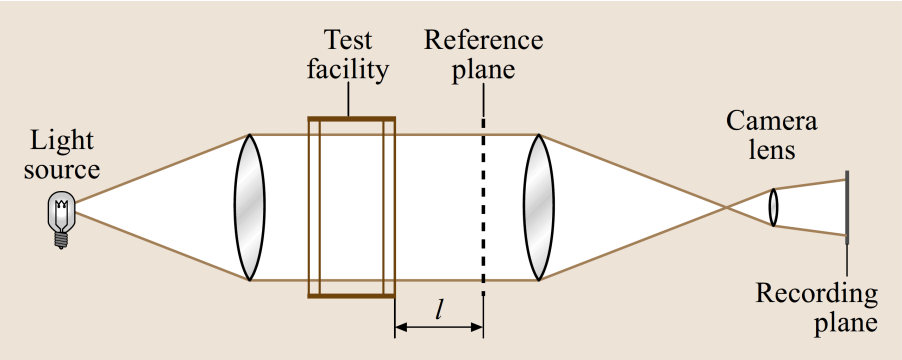

Figure 5: Schematic of shadowgraph setup [2].

4 Experiments

In this laboratory exercise, the experiments are performed with three different flow Mach numbers around the wedge, *i.e.* the Mach number in state 2, M_2. In all the experiments, the temperatures of the different gases in driver and driven sections are assumed to be 300 K (room temperature).

4.1 Experiment 1: Subsonic M_2

The time trace of the measured pressure signals from the oscilloscope are found in "Osiclloscope_traces.pdf". The measured pressure value in state 2 after the incident shock arrival at the wedge (t_w in Figure 2), p_2, as well as the initial driven section pressure, p_1, are indicated on the plot. From the pressure ratio p_2/p_1, the incident shock Mach number, M_s can be obtained as

$$M_s = \frac{c_s}{a_1} = \left[\frac{\gamma_1 + 1}{2\gamma_1}\left(\frac{p_2}{p_1} - 1\right) + 1\right]^{\frac{1}{2}}.$$

The equation is derived from the three governing equations mentioned in the Section 2 and the ideal gas law.

The Mach number behind the incident shock, $M_2 = u_2/a_2$, is determined using the normal shock relations. The continuity equation gives the velocity behind the incident shock, u_2, *i.e.* the velocity in state 2 as

$$u_2 = \left(1 - \frac{\rho_1}{\rho_2}\right) c_s.$$

Assuming ideal gas, the speed of sound is given as $a = \sqrt{\gamma RT}$. Hence in state 2, a_2 is calculated as

$$a_2 = \sqrt{\frac{T_2}{T_1}}\, a_1.$$

Using the normal shock jump relations for temperature and density (a table of normal shock properties may be consulted), M_2 is obtained experimentally from the pressure measurement of p_2.

4.2 Experiment 2: Supersonic M_2, $\theta > \theta_{\max}$

The same procedure as in Experiment 1 should be performed to confirm the value of M_2 experimentally.

4.3 Experiment 3: Supersonic M_2, $\theta < \theta_{\max}$

The same procedure as in Experiment 1 and 2 should be performed to confirm the value of M_2 experimentally.

Furthermore, M_2 can be verified from the shadowgraph snapshot using the $\theta - \beta - M$ curves shown in Figure 7. θ is the wedge angle mentioned in Section 3. β is the shock angle and can be measured from the snapshot. To improve accuracy, it is recommended to measure the angle between an oblique shock and the surface of the wedge, then add θ to the measured value. When using the curve to obtain M_2, careful attention needs to be paid to the subscripts: the Mach number ahead of the oblique shock, M_1, in the $\theta - \beta - M$ relation is the Mach number of state 2, M_2.

5 Evaluation of experimental data

5.1 Experiment 1

Target $M_2 = 0.46$

1 **a.** Calculate the M_s required to achieve the target M_2.
b. Calculate the theoretical p_4/p_1 to achieve the obtained M_s.
c. Calculate the actual p_4/p_1 required to achieve the obtained M_s.
Explain why there is a discrepancy between the theoretical and actual values.

2 **a.** Calculate the M_s from the pressure measurement found in "Oscilloscope_trace.pdf"
b. Calculate the M_2 from the M_s obtained experimentally.
How well does it match the target M_2?
c. Open the video file "Exp1.avi".
Explain your observation referring to the obtained M_2 value.

5.2 Experiment 2

Target $M_2 = 1.04$

1 **a.** Calculate the M_s required to achieve the target M_2.
b. Calculate the theoretical p_4/p_1 to achieve the obtained M_s.
c. Calculate the actual p_4/p_1 required to achieve the obtained M_s.

2 **a.** Calculate the M_s from the pressure measurement found in "Oscilloscope_trace.pdf"
b. Calculate the M_2 from the M_s obtained experimentally.
How well does it match the target M_2?
c. Open the video file "Exp2.avi".
Explain your observation referring to the obtained M_2 value.
$\theta - \beta - M$ curve should also be referred.

5.3 Experiment 3

Target $M_2 = 1.34$

1 **a.** Calculate the M_s required to achieve the target M_2.
b. Calculate the theoretical p_4/p_1 to achieve the obtained M_s.
c. Calculate the actual p_4/p_1 required to achieve the obtained M_s.

2 **a.** Calculate the M_s from the pressure measurement found in "Oscilloscope_trace.pdf"
b. Calculate the M_2 from the M_s obtained experimentally
c. Calculate the M_2 by measuring the shock angle from the shadowgraph snapshot "Exp3_snapshot.jpg". Obtain M_2 from both top and bottom wedge angles.
d. Open the video file "Exp3.avi".
Explain your observation referring to the obtained M_2 values.
$\theta - \beta - M$ curve should also be referred.
e. Compare the M_2 values obtained in 3 different ways and the target value. How well do they match? Which value do you think is the most reliable one?

6 Discussion of assumptions

Ideal gas

The assumption of ideal gases is probably relevant at the low Mach numbers, $M_s < 3$, used in the laboratory exercise, because only minor variations in the heat capacity will occur.

Instant valve opening

This has been discussed in detail in the Section 3. Here, some additional aspects are mentioned. The time it takes until stationary shock speed is reached depends on the valve opening. The valve opening also influences the character of the contact surface. In this laboratory exercise, the shock wave is assumed to be fully developed and plane when it passes the pressure sensor and reaches the wedge. But the time delay due to the finite opening time causes the shock wave line in the x -t diagram to be shifted upwards. We also have to consider the mixing in the contact zone due to an imperfect valve opening and thermal gradients which decrease the time of stationary flow around the wedge.

Boundary layer formation

Behind the shock, the gas temperature and velocity are different compared to the situation along the walls and hence boundary layers start to develop as soon as the valve opens. The boundary layer development causes the shock to attenuate, the contact surface to accelerate and the available time for which the flow is constant to diminish. However, these effects are considered to be of minor importance as the shock Mach number is low and the tube is relatively short in our case.

REFERENCES

[1] Anderson JD. Modern compressible flow: with historical perspective. 3rd ed. McGraw-Hill; 2003.

[2] Tropea C, Yarin AL, Foss JF. Springer handbook of experimental fluid mechanics. Springer; 2007.

[3] Mythealias, Available from: https://commons.wikimedia.org/wiki/File:ObliqueShockAngleRelation.png [Accessed 11th May 2020].

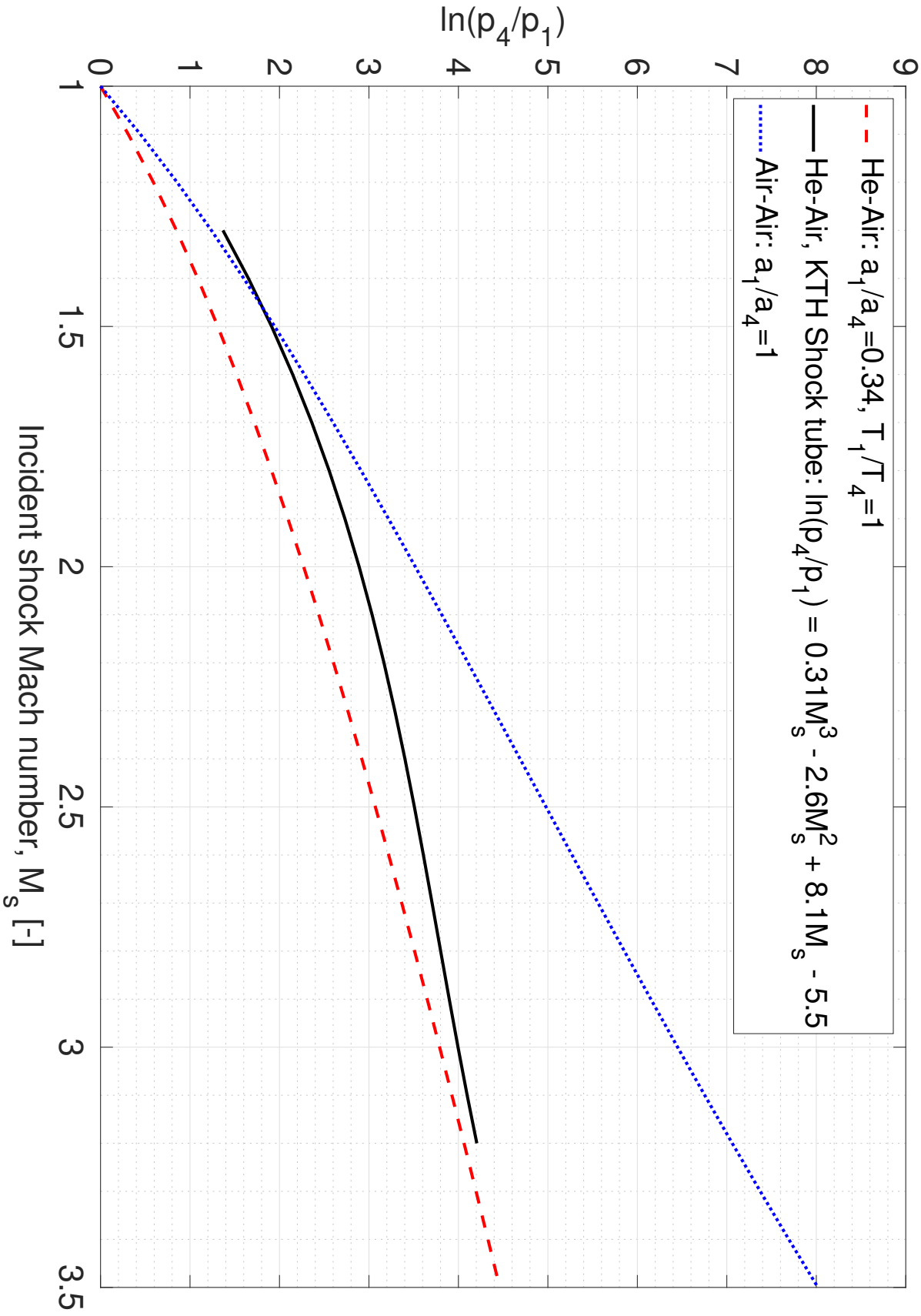

Figure 6: Theoretical and calibration curve for p_4/p_1 vs. M_s relation.

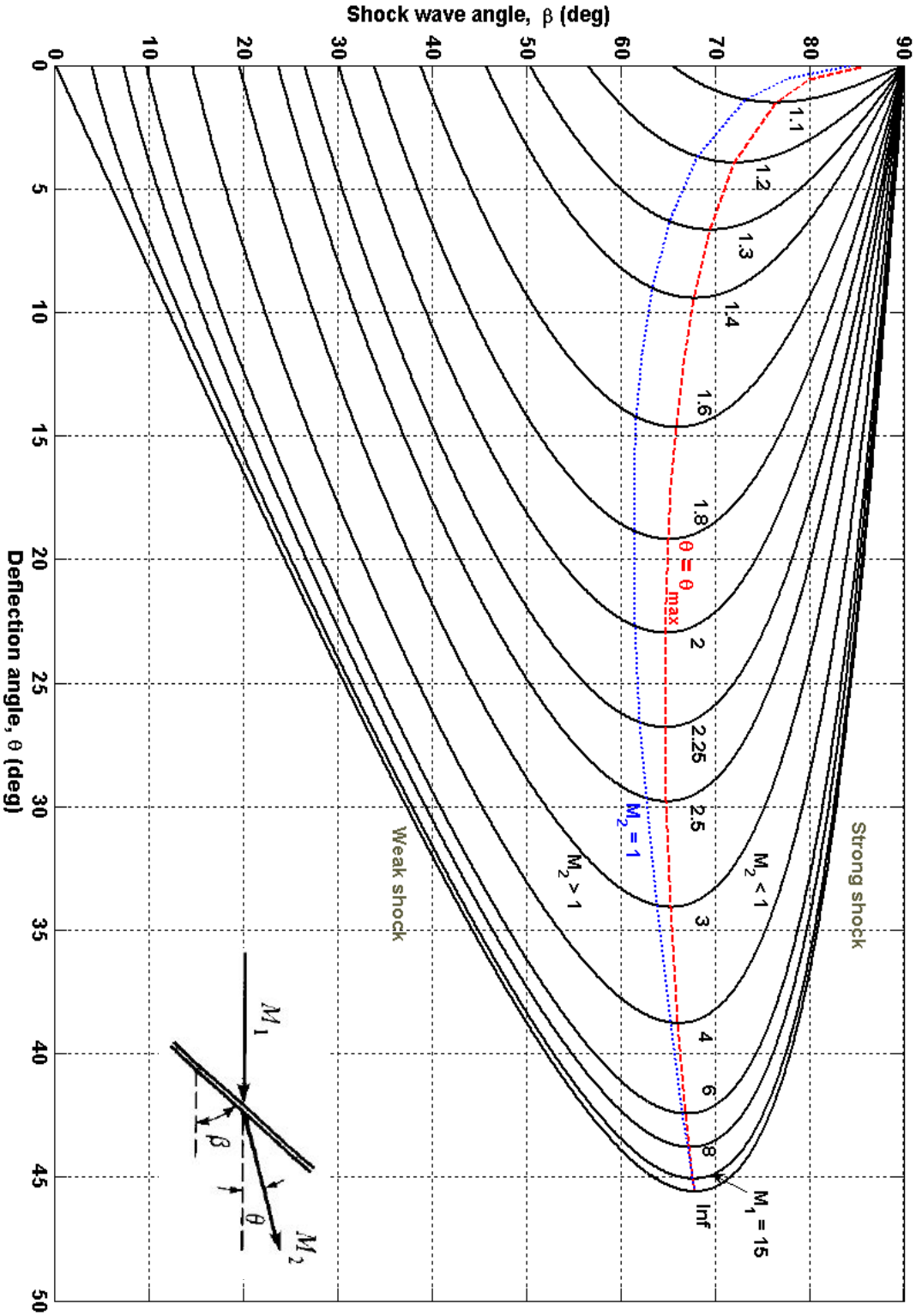

Figure 7: $\theta - \beta - M$ curves. Adapted from Refs. [1&3]